

## Hierarchical Self-Assembly of an Anthracene Derivative in Aqueous Solution

Jie Song,<sup>†,‡</sup> Kang Li,<sup>‡</sup> Pusu Zhao,<sup>‡,\*</sup> and Jianchun Bao<sup>†,\*</sup>

<sup>†</sup>Materials Chemistry Laboratory, Nanjing University of Science and Technology, Nanjing, Jiangsu 210094, People's Republic of China. \*E-mail: songjiesj@163.com

<sup>‡</sup>Jiangsu Key Laboratory for Chemistry of Low-Dimensional Materials, Huaiyin Normal University, Huaian, Jiangsu 223300, P.R. China. \*E-mail: zhaopusu@qust.edu.cn

Received December 6, 2010, Accepted February 21, 2011

**Key Words :** Organic compound, Crystal structure, Crystal growth, Optical properties

Assembly of functional nanoscale building blocks into hierarchical superstructures or complex functional architectures has attracted increasing attentions because of their novel electronic and optical properties in material chemistry and nanoscience.<sup>1-3</sup> Nanotubes, nanowires, nanorods and nanobelts, as a very unique class of one-dimensional (1D) nanoscale building blocks, can be ordered and rationally assembled into appropriate two- or three-dimensional architectures, which are expected to display novel functions for the development of advanced devices.<sup>4-7</sup> Recently, some investigations on assembling nanorods/nanowires building blocks into 2D or 3D complex superstructures have been reported.<sup>7-10</sup> As a powerful tool for creating designed nanomaterials, molecular self-assembly is showing ever increasing importance in chemistry, material science, life science, and nanotechnology.<sup>11-14</sup> Amphiphilic molecules, consisting of hydrophobic and hydrophilic moieties, can self-assemble into highly organized aggregates with one-dimensional nanostructures such as nanowires,<sup>15</sup> nanorods,<sup>16,17</sup> nanotubes,<sup>18-20</sup> and nanofibers.<sup>21-24</sup> Although there have many successful examples in the fabrication of three-dimensional self-organization architectures, it has been a great challenge in the fabrication of the hierarchical architectures with well-defined and highly ordered nanostructures from 1D organic nanomaterials based on low-molecular-weight compounds.<sup>25-27</sup> Most self-assembling one-dimensional materials are macroscopically disordered and difficult to self-assemble into order structures due to the interference of randomly oriented highly anisotropic one-dimensional structures.<sup>26</sup>

In this paper, we wish to give a report about a new kind of amphiphilic molecule material of 4-(2,3,6,7-tetramethoxy-9-(pyridin-4-yl) anthracene-10-yl) pyridine (TPAP), including its single crystal structure and its prickly microspheres by simply controlling the self-assembly process in aqueous solution. Among the polycyclic aromatic hydrocarbons, anthracene and its derivatives have been extensively investigated due to bimolecular photochemical and photochromic properties that can be used in the design of optical, electronic, or magnetic switches.<sup>28</sup> Therefore, TPAP has been selected as the self assembly monomer to study the self-assembly behavior. Such complex architectures are undoubtedly interesting in understanding the self-assembling of hierarchical superstructures and helpful to prepare functional architec-

tures.

X-ray single crystal diffraction indicates that the crystal structure of TPAP crystallizes in triclinic system, space group *P*-1, with lattice parameters  $a = 6.3200(13)$  Å,  $b = 9.5500(19)$  Å,  $c = 9.880(2)$  Å,  $\alpha = 85.05(3)^\circ$ ,  $\beta = 84.31(3)^\circ$ ,  $\gamma = 81.55(3)^\circ$ ,  $V = 585.4(2)$  Å<sup>3</sup>,  $M_r = 452.49$  (C<sub>28</sub>H<sub>24</sub>N<sub>2</sub>O<sub>4</sub>),  $Z = 1$ ,  $D_c = 1.284$  g/cm<sup>3</sup>,  $\mu = 0.086$  mm<sup>-1</sup>,  $F(000) = 238$ , GOF = 1.019,  $R_1 = 0.0527$ ,  $wR_2 = 0.1168$ . A displacement ellipsoid plot with the atomic numbering scheme is shown in Figure 1.

The single crystal structure of TPAP contains a 4-(2,3,6,7-tetramethoxy-9-(pyridin-4-yl) anthracene-10-yl) pyridine molecule, with an inversion center locating at the anthracene ring center. All of the bond lengths and bond angles in anthracene ring, two pyridyl rings and four methoxyl groups are in the normal range. Except the atoms C(2) and C(2A), the other twenty non-hydrogen atoms from anthracene ring and four methoxyl groups define a plane *P*1 with the biggest deviation being 0.068 Å for both C(1) and O(1A) atoms. The dihedral angle between the pyridyl ring and *P*1 is 71.70(2)°.

X-ray powder diffraction pattern of TPAP prickly structures is shown in Figure 2. The diffraction peaks in Figure 2 reveal that the TPAP prickly structures are crystalline.

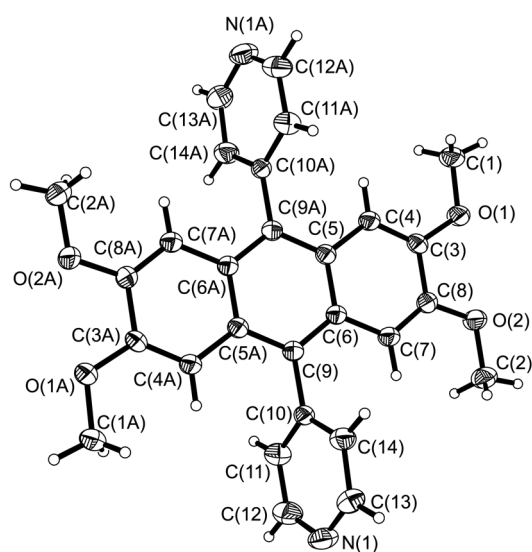


**Figure 1.** The molecular structure with the atomic numbering for TPAP.

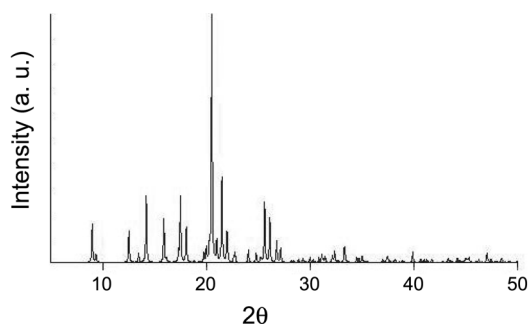


**Figure 2.** X-ray powder diffraction pattern of TPAP.

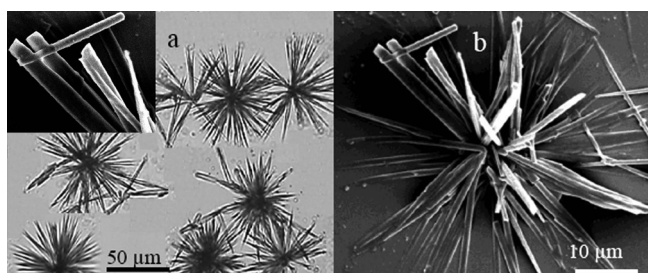


**Figure 3.** Optical micrograph of TPAP from aqueous solution deposition on a glass vessel (a), FE-SEM images of a single self-assembled sample cast from aqueous solution (b).

The panoramic morphology of TPAP given in Figure 3(a) shows that the product consists of entirely hierarchically prickly structures with a diameter of 60–70  $\mu\text{m}$ . A magnified SEM image of a fibrous part of the assemblage is inserted in the Figure 3(a) as an inset, it is found that the fibrous part of the assemblage are many needle-like rods. The high-magnification field-emission scanning electron microscopy (FE-SEM) image of the typical self-assembled hierarchical structure is given in the Figure 3(b). It can be seen that each prickly structure is made of many needle-like rods, which are spokewise and projected from a common central zone. The diameters and lengths of these rods are 0.8–1  $\mu\text{m}$  and 30–40  $\mu\text{m}$ , respectively, which are varied by the reaction time.

To understand the formation mechanism of these hierarchical structures, time-dependent experiments are carried out. A spot of solution of TPAP is taken from the system and the growth of prickly structures is monitored with optical microscopy (see Figure 4). After the deionized water is added to the solution, the diffused particles quickly self-assemble into needle-like rods. With an increase in the self-assembled time, a large number of the needle-like rods are produced, and then quickly move around in the solution. When the floating rods encounter one another, they hold up the movement of one another and start to conglutinate at their thick ends and further develop into prickly superstructures. By further prolonging the self-assembled time to 60 s, the prickly structures based on the uniform rods can be obtained and stop movement, which mainly caused by non-covalent interactions such as  $\pi$ - $\pi$  intercalation. The amphiphilic properties along with the anthracene ring play an important role in the self assembly process of the prickly

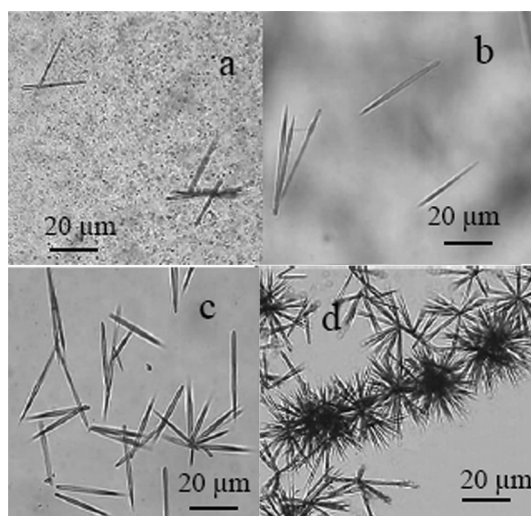


**Figure 4.** Time-lapse optical micrographs of growth video after (a) 5, (b) 20, (c) 40 and (d) 60 seconds in aqueous solution in a glass vessel.

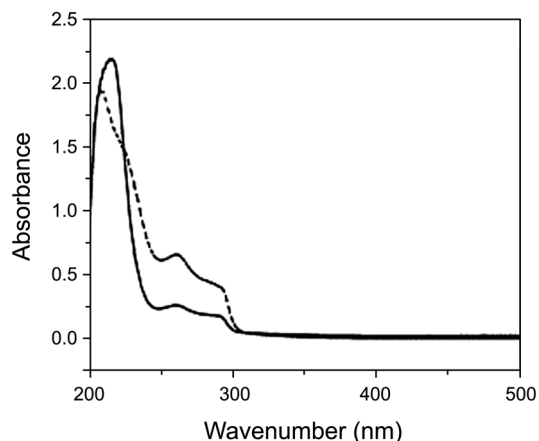


**Figure 5.** UV-vis absorption spectra of TPAP ( $1 \times 10^{-5}$  M) molecularly dissolved in ethanol solution (dotted line) and in the aggregate state dispersed in 2:1 water/ethanol (black solid line).

structures.

UV-vis absorption spectra of the self-assembled TPAP are shown in Figure 5. When TPAP is dissolved in ethanol solvent, it exhibits an intensive absorption peak at about 220 nm and an extensive band from about 250 nm to 300 nm, which are all in the range of ultraviolet region. Upon adding water to the ethanol of TPAP, although all of the absorption bands are still in the ultraviolet region, the absorption peak at 220 nm becomes enhanced, broadening and has some red-shift, while the intensities of absorption band from 250 nm to 300 nm become weak. The above phenomena maybe result from the extended aggregate state formation<sup>29</sup> of TPAP in water/ethanol system and the excited state  $\pi$ -stacking delocalization<sup>30</sup> in TPAP. Moreover, since water molecule is a better hydrogen-bond donor than ethanol molecule, when water is added into TPAP ethanol solution, more hydrogen-bonds are formed between  $\text{H}_2\text{O}$  and TPAP, namely  $\text{O-H}\cdots\text{N}$  hydrogen bond, which will also lead to the intensity change and some red-shifts of the UV spectra.<sup>31</sup>

## Experimental Section

**Synthesis and Self-Assembly of TPAP.** All chemicals were obtained from a commercial source (J&K Chemical Ltd., Beijing, P.R. China) and used without further purification. According to the literature report,<sup>32</sup> 4-(2,3,6,7-tetramethoxy-9-(pyridin-4-yl) anthracene-10-yl) pyridine (TPAP) was synthesized and the synthetic path is shown in Scheme 1. Yield 40.6%. mp 365.0-365.2 °C. IR:  $\nu$  (cm<sup>-1</sup>) 3060 and 3002 ( $\nu_{C-H}$  of anthracene ring), 2960 and 2834 ( $\nu_{C-H}$  of -OCH<sub>3</sub>), 1610-1462 ( $\nu_{C=C}$  of anthracene ring and  $\nu_{C-H}$  of pyridyl ring), 1233-1098 ( $\nu_{C-O}$ ), 1035 ( $\nu_{C-N}$  of pyridyl ring), 891-790 ( $\nu_{C-H}$  of pyridyl ring), 752 ( $\delta_{C-H}$  of phenyl ring). <sup>1</sup>H NMR (400 MHz, DMSO)  $\delta$  3.71(s, 12H, -CH<sub>3</sub>), 6.88 (s, 4H, -CH of anthracene ring), 7.60 (d, 4H, -CH of pyridyl ring), 8.62(d, 4H, -CH of pyridyl ring).

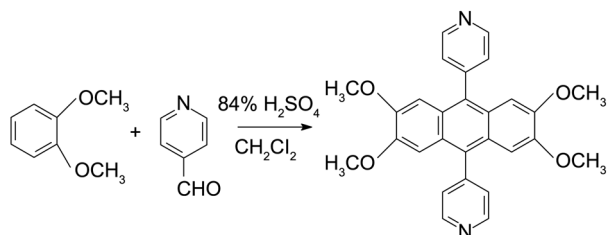
For the compound of TPAP, single crystals suitable for X-ray measurements were obtained by recrystallization from ethanol at room temperature.

IR spectra (4000-400 cm<sup>-1</sup>), as KBr pellets, were recorded on a Nicolet FT-IR spectrophotometer. <sup>1</sup>H-NMR spectra were recorded on a Bruker model DRX 500 spectrometer in DMSO.

The as-synthesized TPAP is soluble in ethanol, acetone, THF, and so on. In a typical synthesis of TPAP picky microspheres, the 0.015 g of TPAP is added into 5.0 mL ethanol and heated at 50 °C until the TPAP is absolutely dissolved. The TPAP solution is cooled down to room temperature, and then 10.0 mL deionized water is slowly added without stirring. When the deionized water is added slowly to the TPAP solution, a white precipitate appeared quickly. The assembly behavior is revealed in the course of direct in situ monitoring of its growth with optical microscopy and field-emission scanning electron microscopy.

The morphology of the prepared samples in 2:1 water/ethanol is investigated with optical microscopy (OM, angel, AQ-2010B, China) and field-emission scanning electron microscopy (FE-SEM, JSM 6700F, Japan). UV/vis absorption spectra are carried out with carry-500 UV-VIS-NIR.

**Crystal Structure Determination.** The diffraction data were collected on a Enraf-Nonius CAD-4 diffractometer with graphite-monochromated Mo-K $\alpha$  radiation ( $\lambda = 0.71073$  Å,  $T = 293$  (2) K). The technique used was  $\omega$  scan with limits 2.08 to 28.34°. The structure of the TPAP was solved by direct method and refined by least squares on  $F^2$  by using the SHELXTL<sup>33</sup> software package. All non-hydrogen atoms were anisotropically refined. All of the hydrogen atom



**Scheme 1.** Synthetic path for the TPAP.

positions were fixed geometrically at calculated distances and allowed to ride on the parent carbon atoms. The molecular graphics were plotted using SHELXTL. Atomic scattering factors and anomalous dispersion corrections were taken from International Tables for X-ray Crystallography.<sup>34</sup>

**Supplementary Data.** Crystallographic data for the structure reported here have been deposited with Cambridge Crystallographic Data Center (Deposition No. CCDC-808858). The data can be obtained free of charge via [www.ccdc.cam.ac.uk/conts/retrieving.html](http://www.ccdc.cam.ac.uk/conts/retrieving.html) (or from the CCDC, 12 Union Road, Cambridge CB2 1EZ, UK; fax: +441223 336033; e-mail: [deposit@ccdc.cam.ac.uk](mailto:deposit@ccdc.cam.ac.uk)).

**Acknowledgments.** This work was supported by Jiangsu Key Laboratory for Chemistry of Low-Dimensional Materials P. R. China (JSKC10078) and Huaian Science & Technology Bureau, Jiangsu Province, P.R. China (HAG2010027).

## References

1. Yu, S. H.; Antonietti, M.; Cölfen, H.; Hartmann, J. *Nano. Lett.* **2003**, *3*, 379-382.
2. Wu, J.; Duan, F.; Zheng, Y.; Xie, Y. *J. Phys. Chem. C* **2007**, *111*, 12866-12871.
3. Zhou, C.; Han, J.; Song, G.; Guo, R. *Macromolecules* **2007**, *40*, 7075-7078.
4. Bok, H. M.; Kim, S.; Yoo, S. H.; Kim, S. K.; Park, S. *Langmuir* **2008**, *24*, 4168-4173.
5. Gu, Z.; Zhai, T.; Gao, B.; Sheng, X.; Wang, Y.; Fu, H.; Ma, Y.; Yao, J. *J. Phys. Chem. B* **2006**, *110*, 23829-23836.
6. Shi, H.; Wang, X.; Zhao, N.; Qi, L.; Ma, J. *J. Phys. Chem. B* **2006**, *110*, 748-753.
7. Mao, Y.; Kanungo, M.; Hemraj-Benny, T.; Wong, S. S. *J. Phys. Chem. B* **2006**, *110*, 702-710.
8. Feng, Y.; Lu, W.; Zhang, L.; Bao, X.; Yue, B.; Lv, Y.; Shang, X. *Cryst. Growth Des.* **2008**, *8*, 1426-1429.
9. Li, Z.; Ding, Y.; Xiong, Y.; Xie, Y. *Cryst. Growth Des.* **2005**, *5*, 1953-1958.
10. Yao, W.; Yu, S.; Liu, S.; Chen, J.; Liu, X.; Li, F. *J. Phys. Chem. B* **2006**, *110*, 11704-11710.
11. Zhang, X.; Chen, Z.; Würthner, F. *J. Am. Chem. Soc.* **2007**, *129*, 4886-4887.
12. Kol, N.; Abramovich, L. A.; Barlam, D.; Shneck, R. Z.; Gazit, E.; Rousoo, I. *Nano. Lett.* **2005**, *5*, 1343-1346.
13. Tian, Y.; He, Q.; Tao, C.; Li, J. *Langmuir* **2006**, *22*, 360-362.
14. Kim, J. K.; Lee, E.; Jeong, Y. H.; Lee, J. K.; Zin, W. C.; Lee, M. *J. Am. Chem. Soc.* **2007**, *129*, 6082-6083.
15. Morikawa, M.; Yoshihara, M.; Endo, T.; Kimizuka, N. *J. Am. Chem. Soc.* **2005**, *127*, 1358-1359.
16. Schwab, A. D.; Smith, D. E.; Bond-Watts, B.; Johnston, D. E.; Hone, J.; Johnson, A. T.; de Paula, J. C.; Smith, W. F. *Nano Lett.* **2004**, *4*, 1261-1265.
17. Schwab, A. D.; Smith, D. E.; Rich, C. S.; Young, E. R.; Smith, W. F.; de Paula, J. C. *J. Phys. Chem. B* **2003**, *107*, 11339-11345.
18. Yang, W. Y.; Lee, E.; Lee, M. *J. Am. Chem. Soc.* **2006**, *128*, 3484-3485.
19. Wang, Z.; Medforth, C. J.; Shelnut, J. A. *J. Am. Chem. Soc.* **2004**, *126*, 16720-16721.
20. Wang, Z.; Medforth, C. J.; Shelnut, J. A. *J. Am. Chem. Soc.* **2004**, *126*, 15954-15955.
21. Hsu, L.; Cvetanovich, G. L.; Stupp, S. I. *J. Am. Chem. Soc.* **2008**, *130*, 3892-3899.
22. Hung, A. M.; Stupp, S. I. *Nano Lett.* **2007**, *7*, 1165-1171.

23. Mille, M.; Lamere, J. F.; Rodrigues, F.; Fery-Forgues, S. *Langmuir* **2008**, *24*, 2671-2679.
  24. Bull, S. R.; Guler, M. O.; Bras, R. E.; Meade, T. J.; Stupp, S. I. *Nano Lett.* **2005**, *5*, 1-4.
  25. Seo, M.; Seo, G.; Kim, S. *Angew. Chem. Int. Ed.* **2006**, *45*, 6306-6310.
  26. Genson, K. L.; Holzmueller, J.; Ornatska, M.; Yoo, Y. S.; Par, M. H.; Lee, M.; Tsukruk, V. V. *Nano Lett.* **2006**, *6*, 435-440.
  27. Wang, Z.; Li, Z.; Medforth, C. J.; Shelnutt, J. A. *J. Am. Chem. Soc.* **2007**, *129*, 2440-2441.
  28. Cakmak, O.; Erenler, R.; Tutar, A.; Celik, N. *J. Org. Chem.* **2006**, *71*, 1795-1801.
  29. Che, Y.; Datar, A.; Balakrishnan, K.; Zang, L. *J. Am. Chem. Soc.* **2007**, *129*, 7234-7235.
  30. Jiang, H.; Sun, X.; Huang, M.; Wang, Y.; Li, D.; Dong, S. *Langmuir* **2006**, *22*, 3358-3361.
  31. Saeed, Z.; Hajar, R.; Robabeh, A. *Spectrochim. Acta A* **2010**, *77*, 994-997.
  32. Goossens, R.; Smet, M.; Dehaen, W. *Tetrahedron Lett.* **2002**, *43*, 6605-6608.
  33. Sheldrick, G. M. *SHELXTL, v5 Reference Manual*; Siemens Analytical X-Ray Systems: Madison, WI, 1997.
  34. Wilson, A. J. *International Table for X-Ray Crystallography*; Kluwer Academic: Dordrecht, The Netherlands, 1992; Vol. C, Tables 6.1.1.4 (pp 500-502) and 4.2.6.8 (pp 219-222), respectively.
-